

Coupling of sentiment-polarity and opinion in discrete topologies

Author: Mario Díez Hermoso

Facultat de Física, Universitat de Barcelona, Diagonal 645, 08028 Barcelona, Spain.

Advisors: Emanuele Cozzo, Albert Díaz, Luce Prignano

Abstract: We present here an agent-based model determined by integrate and fire oscillators. These oscillators fire whenever they reach a certain threshold value of its phase and thus interact with their neighbours within an established range, attracting them a definite distance. The behaviour of these agents directly depends on this range of interaction, determining whether the final state becomes completely sparse (fragmentation of opinion), formed by one big cluster (consensus), or halfway between.

I. INTRODUCTION

Social dynamics are of great importance for our understanding of human interactions, since a statistical approach can give us information about the collective phenomena emerging from the relations among individuals [1]. In order to study the nature of social interactions, a large number of models have been studied among physicists. An example of these is the voter model: analogue to the Ising model's formalism, each individual is assigned a spin that represents binary opinions.

Since the early eighties, many bounded-confidence models (initially introduced by [2]) have been proposed. These models consider opinions as continuous variables (in contrast to the binary opinion of the voter model), and the interaction between individuals only takes place if their opinion is close enough.

To achieve a more realistic description, sentiment-polarity can also be taken into account through a mean field approximation [3]. Hence, a coupling of sentiment-polarity and opinion is obtained. In this model, the agents contribute to the global dynamics whenever its arousal exceeds a certain threshold. However, the non-linear nature of its equations can lead to difficulties.

In the present thesis we make a step further, introducing integrate and fire oscillators [4]. Each of this oscillators has a random initial phase assigned (that evolves linearly in time), and interacts with those who are close enough to it whenever its value is greater than a specific threshold, just as the agent-based models given by [3].

In addition, we introduce an attraction parameter. The aim of this parameter is to suggest that an interaction between neighbouring agents should bring them even closer. This model should not be regarded as a realistic description of how sentiment-polarity drives human opinion. Rather, is an exploratory characterisation of the main features of the interplay between the oscillators belonging to the system and its evolution in time.

II. A CLOSER LOOK AT THE MODEL

Let us consider a setting consisting of a population of N agents to which a random initial position in a square of dimensions $\Lambda \times \Lambda$ is assigned. These two dimensions correspond to opinion and sentiment-polarity, the squared-shape attribute being a convention. Each one of the agents has a random phase $\phi \in [0, 1]$ that evolves in a linear manner with time and has a period τ , being set to zero whenever $t = \tau$. The phase evolution is given then by [4]:

$$\frac{d\phi_i(t)}{dt} = \frac{1}{\tau}. \quad (1)$$

Henceforth, $\tau=1$ will be considered. A fixed range of interaction (or radius) R is designated to each agent (equal for all of them). We can then define a neighbour as an agent that lies within a distance $d < R$ from another one. We can construct a graph out of these nodes, assigning a link whenever two of them are neighbours. Another variable that will be useful is the average connectivity k of a graph, defined as the average number of links (i.e. neighbouring oscillators) per node. Depending on this radius, the number of neighbours of an agent (and hence k) may vary significantly, ranging from few or even none for small ranges, to the complete set of oscillators belonging to the system for larger ones.

As we shall see shortly, two different types of interaction between agents take part in the model. The first has inherited the basic dynamics of the phases from [5]. The second one has an influence in the positions of the agents, and consists in the attraction between them.

Each time $\phi_i(t) = 1$, the i^{th} agent fires, its phase being set to zero. As a part of the interplay in the firing event, all the neighbours of the firing agent increase their phase by a factor ϵ , called coupling constant. If we label the affected agent as j , i being the one that fires, $\phi_i(t^*) = 0$; $\phi_j(t^*) = \phi_j(t) \cdot (1 + \epsilon)$, where $*$ denotes the time immediately after the firing event. Interacting *simultaneously* with $n \leq N$ oscillators would lead to $\phi_j(t^*) = \phi_j(t) \cdot (1 + \epsilon)^n$. During the firing event, if the j^{th} phase's updated value is greater than the established threshold, its phase is set to zero and it fires to its neighbours as well. This process will continue until $\phi_i < 1 \forall i$,

the time running again and only stopping when the next firing event occurs. It is important to notice that an agent can be affected in a firing event if and only if it lies within the range of interaction of at least one of the firing agents, its phase remaining unaltered otherwise. In order to help to elucidate the time matter we will make use of the stroboscopic time $T \in \mathbb{N}$ [5], that increases by one each time an assigned reference agent, say r , fires ($\phi_r = 1$). We say that a certain amount of oscillators are synchronised when they have the same phase (i.e., they fire at once).

Apart from the interactions regarding their phases, we introduce a new dynamical feature: the attraction between agents in the $\Lambda \times \Lambda$ space. We define *trigger neighbours* as those neighbours of an agent that fire at it at once. Thereby, the number of trigger neighbours of an agent in a firing event is always less or equal to that of neighbours, the equality holding when all of the neighbours are synchronised. Let $n \leq N$ then be the number of trigger neighbours shooting the agent j *simultaneously*. As a general rule for motion, this affected agent is attracted a distance α towards the centroid formed by all of them (including j itself). However, if the distance α travelled by j exceeds that of the centroid, the fired agent will not move further, staying on the latter's position. If we define $\omega = \min(\alpha/d_{C_j}, 1)$ being d_{C_j} the distance between the j^{th} oscillator and the centroid considered, the computation of its new position in a general case is given by:

$$\begin{cases} x_{j^*} = x_j + \omega \frac{\sum_{i=v_1}^{i=v_n} (x_i - x_j)}{n+1} \\ y_{j^*} = y_j + \omega \frac{\sum_{i=v_1}^{i=v_n} (y_i - y_j)}{n+1} \end{cases} \quad (2)$$

where the second term in both equations could be seen as the projections of $\min(\alpha, d_{C_j})$ on their respective axis. By construction, no oscillator can move beyond the centroid formed by the trigger neighbours and the affected agent. Hereafter, the focus will be put on the case $\alpha \ll R$, since we want all the steps to be of the same size with the exception of the last one (of size d_{C_i}), that is shorter than the rest.

Therefore, the dynamics of the system start in a scenario where random *opinions* (x) and *sentiment polarities* (y) as well as asynchronous phases are assigned to the N oscillators. This initial state evolves towards a configuration in which these agents clusterize into a number $C_f \leq N$ of consensus groups. In the final state, the agents belonging to the same consensus group will share the same position (x, y) and fire synchronously.

Taking into account the dynamics stated, we introduce the relaxation time $T_{rel} \in \mathbb{N}$ as the stroboscopic time at which, for the first time, interactions do not affect the position of any of the agents involved. At that time, the agents belonging to the same cluster have just collapsed in the same position (x, y) and there is no more movement in the system.

In order to compute T_{rel} numerically we introduce a tolerance parameter μ . Within this approach, two oscillators whose distance is lower than this parameter are considered to be located at the same position. With this criterion, we can assume that relaxation is achieved when the distance between any pair of agents satisfies the previous condition. Hence, if $|d_{ij}(T+1) - d_{ij}(T)| < \mu \forall i, j \in N$, we consider that relaxation is achieved.

In the next sections, we will first provide a preliminary description of the effects that the interaction range R has on the relaxation time T_{rel} and show right after the evolution of the interaction patterns between the agents.

III. RELAXATION TIME

The relaxation time can be regarded as the time it takes to the last agent to reach its final position. Since the movement of this agent takes place in the $\Lambda \times \Lambda$ space, this time directly depends on the dimensions of the system (Λ). The range of interaction R will also play an important role in terms of relaxation, because it provides a value for the maximum distance between interacting units. The step length α (that can be seen as a velocity: the distance travelled for an oscillator between T and $T+1$) is a relevant parameter as well, determining the time needed for an agent to reach the stationary state's position. T_{rel} also depends on both the number of oscillators N and the coupling parameter ϵ . N , on the one hand, determines the number of interactions that take place before relaxation is achieved. On the other hand, ϵ influences how fast synchronisation is achieved, and this may lead to different behaviour depending on whether the trigger neighbours are firing simultaneously or not.

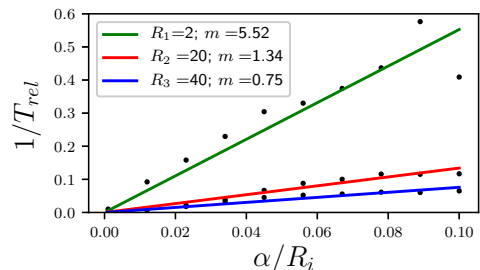


FIG. 1: $1/T_{rel}$ vs α normalised with a fixed value of R_i . We see that as long as $\alpha \ll R_i$ is verified, the relaxation time is inversely proportional to α , m accounting for the slope of the fit (solid line). For the sake of clarity, errors have not been included.

In Figure 1 we plot $1/T_{rel}$ as a function of α/R for three fixed values of R . We find a proportional dependence different for each value of R , hence confirming that α acts as a velocity parameter in the system.

From now on, where not otherwise indicated, we set $\epsilon = 0.02$, $\Lambda = 100$, $N = 50$, $\alpha = 0.1$ and $\mu = 0.005$, and average over 200 randomised realisations of the process.

Figure 2 shows the dependence of T_{rel} on R . Three different regions can be identified, starting with a slow growth for small R , a roughly linear increase of T_{rel} for intermediate radius, and finally reaching a constant value for larger ones. The average fraction of the biggest cluster's size in the initial configuration as a function of R is also represented, so as to show that its behaviour is similar to that of T_{rel} .

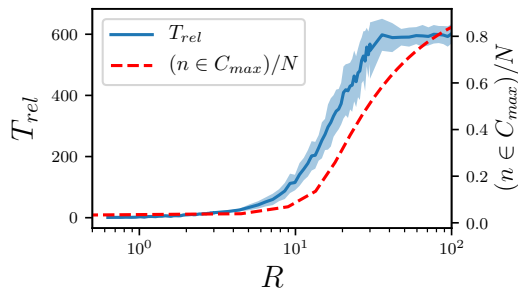


FIG. 2: Relaxation time (left y-axis) and average fraction of the largest cluster's size in the initial configuration (right y-axis) as a function of the radius, the shaded area accounting for the standard deviation.

Let us now introduce the concept of a connected component, defined as a subgraph in which any two nodes are connected to each other by paths, and which is connected to no more nodes in the graph.

On a first examination, we can see that the percolation transition that exists in the network of interaction when R reaches a certain threshold value R_p plays a key role in the distinction between these three regions. In the framework of percolation theory, this threshold value is defined as the minimum radius that allows the system to display a giant component of the order of the system's size with a probability $p \neq 0$.

Thereby, the division of these three regions is done as follows:

1. Very small values of R , where the existence of a giant component is not possible.
2. Intermediate values of R . Here, the expected size of the largest component increases with the radius.
3. Very large values of R . In this scenario, the probability of finding a component of the same size of the system is almost 1.

With the aim of seeing the main differences between these regions, we plotted in figure 3 the trajectories in the $\Lambda \times \Lambda$ space of both the reference agent and the centroid of the sub-system made up by this agent and its trigger neighbours. These trajectories account for each of the three distinct regions, and has been obtained for an individual realisation, setting all the initial phases equal to 1.

In figure 3(a) we see no significant change in time - neither by the reference agent nor its centroid-. In fact, if we decreased the value of R even more, the oscillator would not interact with anyone else (the centroid's position corresponding to that of the agent), and so movement would not be possible. In the case shown in 3(b), we can perceive that while the agent travels a long distance during the relaxation time, the centroid does not move that much. This is because in this scenario the agents form a fully-connected graph and the centroid's position takes into account all of them at each step. Regarding the third framework shown in figure 3(c), we see that the centroid moves as much as the agent at each stroboscopic cycle. We expect then a less predictable evolution determined as a last resort by its initial configuration.

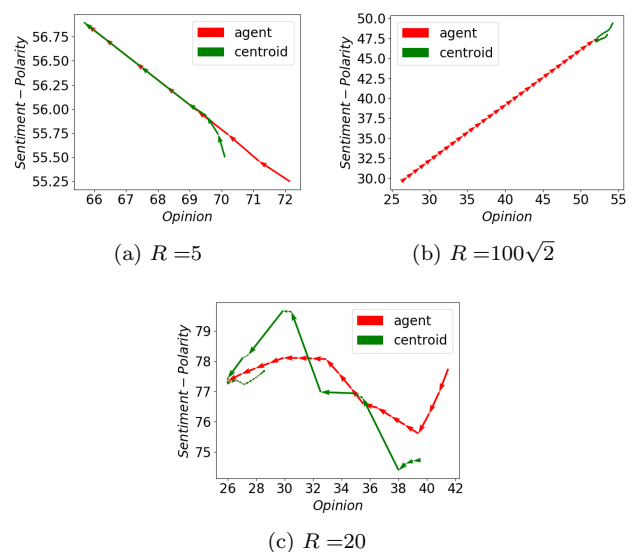


FIG. 3: Trajectory of the reference agent (red) and the centroid formed by their trigger neighbours and itself (green) for the three characteristic regions. In this simulation, the same initial phase ($\phi = 1$) for all agents is given, assuming synchronisation from the beginning. Here we have used $\alpha = 1$.

A. Far below percolation, $R \ll R_p$

For very small values of R , most of the agents are isolated, and so there is no significant interaction between them. However, the existence of groups of two or even three-agent clusters in the initial configuration is possible as well. Because isolated agents do not interact with the rest, the relaxation time only depends on these two-node and three-node subgraphs. Moreover, due to both the sparse connectivity of this regime and the low average number of nodes per cluster, the time at which the relaxation condition is satisfied is not that long. As figure

4 denotes, the theoretical dependence [6]

$$T_{rel} \approx \frac{R}{2\alpha} \cdot [1 - \exp(-\pi R^2 N^2 / 2L^2)], \quad (3)$$

does not differ significantly from the numerical results. As we increase R , T_{rel} approaches a linear dependence on the interaction radius.

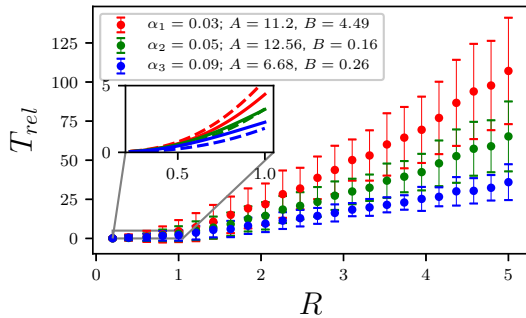


FIG. 4: Dependence of the relaxation time with the radius far below the percolation threshold for different values of α . The dashed lines in the inset accounts for the theoretical dependence, whereas the solid lines are the best fit of the curve $T_{rel} = A \cdot R[1 - \exp(-B \cdot R^2)]$ obtained.

B. At the percolation transition $R \approx R_p$

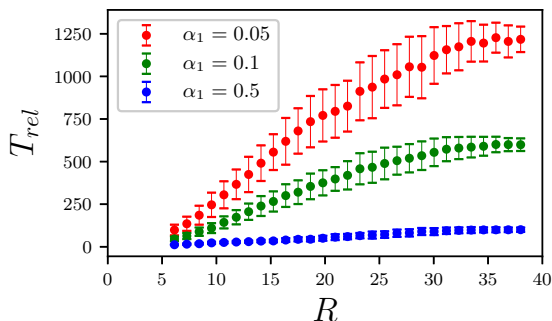


FIG. 5: Relaxation time as a function of radius for values close to the percolation.

In this transition, the size of the connected components changes significantly depending on the realisation, ranging from isolated agents to p -node components ($p \leq N$). This variability of the initial configuration may affect the evolution of the dynamics of the system and thus its relaxation time, as it is shown in figure 5. Because the size of the largest cluster might vary considerably, we expect a wide range of T_{rel} values as well. Studies in Random Geometric Graphs (RGG) [7] have determined the critical average connectivity in a d -dimensional graph and, in particular, for the 2-dimensional case we have $k \approx 4.51$.

Thus, making use of the fraction of the system available for interaction that is $r = \pi R_p^2 / \Lambda^2$ and of a first approach for the average connectivity, $k = (N - 1) \cdot r$ [5], we can obtain the percolation value of the radius in the case we are concerned:

$$k = \frac{\pi R_p^2}{\Lambda^2} (N - 1) \iff R_p \approx \sqrt{4.51 \cdot \frac{\Lambda^2}{\pi(N - 1)}}, \quad (4)$$

from which we obtain $R_p \approx 17.11$ for the fixed values of our simulation (notice that the result $k_p \approx 4.51$ holds only if we assume $N \rightarrow \infty$).

C. Far above the percolation, $R \gg R_p$

Under the conditions $R \gg R_p$, if the radius has the same order of magnitude of Λ , all the agents belong to the same sub-system with probability $p \approx 1$. As it is shown in figure 2, further increasing of the radius in this range does not affect T_{rel} but only changes the density of interaction.

At a sufficient large R , all agents form a fully-connected graph (since the distance between them does not exceed $\sim R$, and so all of them are directly connected). In figure 6 we can see the expected dependence: a proportional increase of T_{rel} as we increase the size of the system Λ .

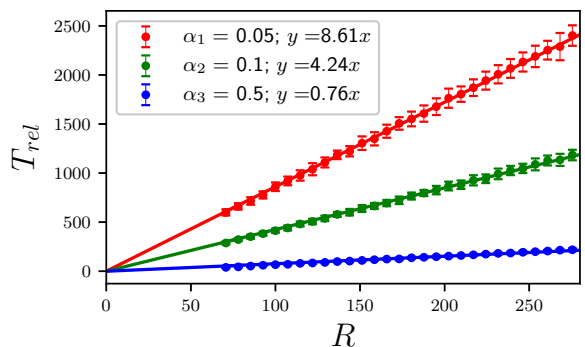


FIG. 6: T_{rel} vs R for different values of α far above the percolation. m accounts for the slope of the linear fit (solid line).

The value of R above which no change can happen (regarding the interaction patterns) is $R_{max} = \Lambda \cdot \sqrt{2}$, since there cannot be agents further away left to interact with. In order to verify $R \sim \Lambda \cdot \sqrt{2}$ for all R shown in figure 6, we varied Λ in the range $[50, 250]$, the condition $\alpha \ll R$ holding at any point. We can observe a linear dependence of T_{rel} on R for values $\alpha < 1$, an increase of radius involving an increase of T_{rel} as well.

IV. EVOLUTION OF THE CONNECTIVITY PATTERNS

Once we have seen the main differences of the three regions regarding relaxation, we shall now take a look at

the principal features of the connectivity patterns, taking a keen interest in the formation of collapsing clusters, which we define as these clusters formed by agents that share the same position $(x,y) \in \Lambda \times \Lambda$ in the final state. As it can be observed in figure 7, far below the percolation value (red) sparse configuration is assured $\forall R$ given the small probability of interaction. In this case there is no change in the number of connected components between the initial and final configuration, which is close to N in both cases. The same happens far above the percolation (yellow), since almost all the simulations begin and end with all the oscillators belonging to the same connected component. In the final state there is only a single collapsing cluster thanks to the large value of R . Near the percolation threshold (green), in contrast, we can see different kinds of evolution for the connected components, some of them becoming collapsing clusters ($\in (1,1)$ in figure 7) in the final state. Nevertheless, depending on the initial configuration, we can in some cases perceive a disintegration tendency, since the final state can have more connected components than the initial one. The essential difference between the transition region and the other two is that in the first one a prediction of the final state is not possible.

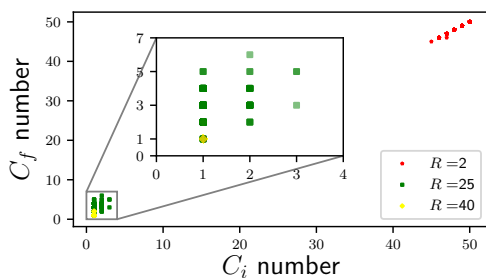


FIG. 7: Number of final connected components as a function of the number of the initial ones for the three regions.

As figure 8 shows, far below from R_p agents are mostly isolated, and the probability of two of them staying in range is very low, the connectivity being almost 0 at any time as a consequence. In contrast, far above R_p there is a tendency of the agents from the same connected component to group, eventually all reaching direct interaction, and so k increases with T . Close to the percolation we can see an intermediate case: the connectivity increases

on average but does not achieve a specific value like in the previous cases. What is common in both $R \gg R_p$ and $R \ll R_p$ - that it is not held for $R \approx R_p$ - is that at sufficient large times the average connectivity reaches a constant value.

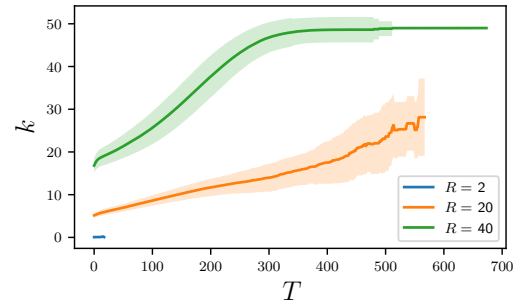


FIG. 8: Average connectivity k of the system as a function of the stroboscopic time T for the three different regions. The shaded area accounts for the standard deviation.

V. CONCLUSIONS

A phenomenological study of the relaxation time as well as the evolution of the connectivity patterns of this model has been done, and two important sum-up conclusions have been obtained:

1. The configuration in the final state mainly depends on the regime of the system, leading to consensus ($R \gg R_p$) or fragmentation of opinion ($R \ll R_p$) separated by an intermediate region, generally less predictable.
2. As regards T_{rel} , the dependence of its value on R exhibits different behaviour if the range of values studied are greater, lower or close to the percolation threshold, given by $R_p \approx 17.11$.

Acknowledgments

I would like to thank Albert Díez for letting me discover the complex system's univers, and Emanuele and Luce for their guidance and support during this thesis. I would especially thank Luce for her commitment and attention whenever I needed, without whom this work would not have been the same.

-
- [1] C. Castellano, S. Fortunato, and V. Loreto, Rev. Mod. Phys. **81**, 591 (2009).
 - [2] G. Deffuant, D. Neau, F. Amblard, and G. Weisbuch, Adv. in Comp. Syst. **3**, 87 (2000).
 - [3] F. Schweitzer, T. Krivachy, and D. Garcia (2019), 1908.11623.
 - [4] R. E. Mirollo and S. H. Strogatz, SIAM J. Appl. Math.

- [5] L. Prignano, O. Sagarra, P. M. Gleiser, and A. Díaz-Guilera, Bif. Chaos **22**, 1250179 (2012), ISSN 1793-6551.
- [6] L. Prignano, <http://www.heuristica.barcelona/DocsLab/SpatialIFOSAttrInt.pdf> (2020).
- [7] J. Dall and M. Christensen, Phys. Rev. E **66** (2002), ISSN 1095-3787.